The Journal of Chemical Physics

Vibration-vibration and vibration-translation energy transfer in H2-H2 collisions: A critical test of experiment with full-dimensional quantum dynamics

S. Fonseca dos Santos, N. Balakrishnan, R. C. Forrey, and P. C. Stancil

Citation: J. Chem. Phys. **138**, 104302 (2013); doi: 10.1063/1.4793472
View online: http://dx.doi.org/10.1063/1.4793472
View Table of Contents: http://jcp.aip.org/resource/1/JCPSA6/v138/i10
Published by the American Institute of Physics.

THE JOURNAL OF CHEMICAL PHYSICS **138**, 104302 (2013)

Vibration-vibration and vibration-translation energy transfer in H_2-H_2 collisions: A critical test of experiment with full-dimensional quantum dynamics

S. Fonseca dos Santos,[1,a)] N. Balakrishnan,[1,b)] R. C. Forrey,[2] and P. C. Stancil[3]
[1]*Department of Chemistry, University of Nevada, Las Vegas, Las Vegas, Nevada 89154, USA*
[2]*Department of Physics, Penn State University, Berks Campus, Reading, Pennsylvania 19610-6009, USA*
[3]*Department of Physics and Astronomy and the Center for Simulational Physics, University of Georgia, Athens, Georgia 30602, USA*

(Received 27 December 2012; accepted 12 February 2013; published online 8 March 2013)

Quantum scattering calculations of vibration-vibration (VV) and vibration-translation (VT) energy transfer for non-reactive H_2-H_2 collisions on a full-dimensional potential energy surface are reported for energies ranging from the ultracold to the thermal regime. The efficiency of VV and VT transfer is known to strongly correlate with the energy gap between the initial and final states. In $H_2(v = 1, j = 0) + H_2(v = 0, j = 1)$ collisions, the inelastic cross section at low energies is dominated by a VV process leading to $H_2(v = 0, j = 0) + H_2(v = 1, j = 1)$ products. At energies above the opening of the $v = 1, j = 2$ rotational channel, pure rotational excitation of the para-H_2 molecule leading to the formation of $H_2(v = 1, j = 2) + H_2(v = 0, j = 1)$ dominates the inelastic cross section. For vibrationally excited H_2 in the $v = 2$ vibrational level colliding with $H_2(v = 0)$, the efficiency of both VV and VT process is examined. It is found that the VV process leading to the formation of $2H_2(v = 1)$ molecules dominates over the VT process leading to $H_2(v = 1) + H_2(v = 0)$ products, consistent with available experimental data, but in contrast to earlier semiclassical results. Overall, VV processes are found to be more efficient than VT processes, for both distinguishable and indistinguishable H_2-H_2 collisions confirming room temperature measurements for $v = 1$ and $v = 2$.
 [http://dx.doi.org/10.1063/1.4793472]

I. INTRODUCTION

Collisional relaxation of rovibrationally excited molecules has long been a topic of considerable theoretical and experimental interest. It is an important process in atmospheric chemistry,[1] astrophysics,[2] hydrogen plasmas, and fusion reactors,[3] and in many environments where non-equilibrium kinetics plays a dominant role. More recently, relaxation of vibrationally excited molecules has received renewed interest in the study of the formation and decay of cold and ultracold molecules.[4–8] For example, in photoassociation [9] and Feshbach resonance[10,11] schemes the vibrational quenching or chemical reaction that follows the formation of the cold molecules is the main source of their depletion. These techniques generally create molecules in high vibrational levels and the quenching mechanisms of such highly vibrationally excited molecules have not yet been fully understood. For theoretical studies that require a quantum mechanical treatment for such systems, the complexity arises from having to incorporate a large rovibrational basis which makes computational studies prohibitively expensive. As a result some recent calculations have used H_2 as a prototype to understand relaxation of highly vibrationally excited molecules.[12,13]

Molecular hydrogen is also an important species in the interstellar medium,[14] for thin film deposition techniques,[15] and in plasma and fusion research.[16,17] For instance, in diamond deposition,[15] hydrogen plasmas are often employed. To understand and improve the deposition process, the corresponding kinetics, including those involving vibrationally excited H_2 are required. Vibrationally excited H_2 is present in low-temperature astrophysical media exposed to shocks and intense ultraviolet radiation, in the boundary region of hydrogen plasma expansions, and in magnetically confined fusion plasmas experiments, such as the International Thermonuclear Experimental Reactor (ITER) which is currently under construction. In fusion plasmas and hydrogen plasma expansions, an important loss mechanism of protons is the charge exchange with H_2.[16] This is an endothermic process which is greatly enhanced by internal excitation of H_2.[18,19] Determination of H_2 rovibrational population in the edge plasma of fusion reactors is thus an important topic in fusion plasma research.[17] This is also an important topic in astrophysics, where H_2 is the dominant coolant in primordial and low-metallicity gas.[20] But even for H_2, with its well separated rovibrational levels, a full quantum mechanical treatment can become quite challenging for excited vibrational levels.

While H_2-H_2 collisions are more amenable to theoretical modeling, experimental studies are difficult and limited to small quanta excitation. This is mostly due to the difficulty in pumping and probing molecules that lack a permanent dipole

a)Electronic mail: sfonseca@ucdavis.edu.
b)Electronic mail: naduvala@unlv.nevada.edu.

moment. Dating back to 1975, Audibert *et al.*[21] measured vibrational relaxation of ortho- and para-H_2 between 40 and 500 K and found the self-relaxation rates to remain identical up to 300 K, beyond which the ortho-ortho collision rate becomes larger. Nearly a dozen years after the experiment of Audibert, Meier *et al.*[22] studied rotational relaxation in vibrationally excited H_2 and D_2 in collisions with H_2, D_2, and He at 300 K. They concluded that the pure rotational rates are in general larger than the corresponding rates in $v = 0$. Kreutz *et al.*[23] reported in 1988 the direct measurements of vibration-vibration (VV) and vibration-translation (VT) rates out of the $v = 2$ vibrational level, also near 300 K. The same year, Farrow and Chandler[24] presented experimental results of rovibrational energy transfer between H_2 molecules colliding in their ground and first excited vibrational levels at 295 K. In 2005, Maté *et al.*[25] reported theoretical and experimental rate coefficients for rotational excitations in para-H_2–para-H_2 collisions between 2 and 110 K. Subsequently, Ahn *et al.*[26] reported experimental rate coefficients for VV transitions in H_2 for $v = 0 - 5$ at 300 K. They investigated both non-resonant VV process such as $H_2(v = 1) + H_2(v = 1) \rightarrow H_2(v = 2) + H_2(v = 0)$ (denoted as (1,1 → 2,0)) and the resonant VV process, $H_2(v = 1) + H_2(v = 0) \rightarrow H_2(v = 0) + H_2(v = 1)$. The resonant VV process involves initially ortho-H_2 in $v = 1$ (primarily in $j = 1$ rotational level) and para-H_2 in $v = 0$ (primarily in $j = 0$, 2 rotational levels). Thus, the VV process involves transfer of vibrational energy from ortho-H_2 to para-H_2. For both processes, the measured rate coefficients were found to be comparable to previous experimental results of Kreutz *et al.*[23] and Farrow and Chandler.[24]

Unfortunately, the available theoretical data are rather limited for VV and VT processes in H_2-H_2 collisions. The most widely quoted results are the semiclassical calculations of Billing and co-workers.[27–30] However, significant discrepancy exists between theory and experiment for both the resonant and non-resonant VV exchange discussed above. For instance, the semiclassical results for the resonant VV process are found to be about a factor of 30 smaller than the measurements of Ahn *et al.*[26] Further, the semiclassical calculations predict the non-resonant VV process (1,1 → 2,0) to be more efficient than the resonant process while the experiments indicate the latter to be about a factor of 2.5 times faster.[26] The discrepancy is attributed to the classical mechanical treatment of rotational motion in the semiclassical approach which is less appropriate for a highly anharmonic molecule such as H_2. More recently, Kelly[31] reported results for VV and VT exchange in H_2-H_2 collisions using a semiclassical approach in which both rotation and vibration are treated quantum mechanically with relative translational motion treated classically. However, the dependence of the H_2-H_2 interaction potential on H-H separations was modeled based on a He-H_2 potential and transition probabilities were computed using first-order perturbation theory. While this approach yielded improved agreement with experiment for the resonant VV process described above the agreement is less satisfactory for other non-resonant VV processes.

The H_2-H_2 system has been the topic of a large number of theoretical investigations over the last two decades with focus both on computing improved interaction potentials[32–37] and on quantum dynamics calculations.[13,38–55] Quantum calculations are the primary source of state-resolved rate coefficients for astrophysical modeling. Excitation of rotational and vibrational levels of H_2 by collisions with H, H^+, He, H_2, and electrons followed by emission of quadrupole radiation is considered to be the main cooling mechanism of the primordial gas. While H_2-H_2 collisions only constitute a subset of the data needed for H_2 cooling, it is one of the more challenging systems for quantum dynamics calculations due to the many degrees of freedom involved in a diatom-diatom interaction. As a result, many of the early H_2-H_2 calculations resorted to the rigid-rotor approximation. However, in the last several years, a number of full-dimensional quantum calculations have been reported within the time-dependent[45,47,49–52] and time-independent[13,44,46,53–55] quantum formalisms. Some of these calculations have adopted the coupled-states approximation,[44–47] which was shown to be reliable. Recent calculations from our group have adopted the full close coupling method within the time-independent quantum formalism[13,53–55] and largely explored interesting features of molecule-molecule collisions at temperatures in the cold and ultracold regimes, where quantum effects play a dominant role. In the course of this work, novel energy transfer mechanisms that lead to exchange of rotational and vibrational quanta between the colliding molecules have been investigated. In particular, in collisions of indistinguishable H_2 molecules (para-para or ortho-ortho), exchange of rotational quanta between the two molecules as in $H_2(v_1, j_1) + H_2(v_2, j_2) \rightarrow H_2(v_1, j_1 + 2) + H_2(v_2, j_2 - 2)$ lead to highly efficient transitions that conserve the total rotational angular momentum of the molecules and nearly conserves the total internal energy.[13,56] Similarly, in collisions of distinguishable H_2 molecules (ortho-para), as in the $H_2(v_1, j_1) + H_2(v_2, j_2) \rightarrow H_2(v_2, j_1) + H_2(v_1, j_2)$ quasi-resonant process, involves the exchange of vibrational quanta between the two molecules while conserving the total rotational angular momentum of the collision pairs.[55] This latter process is a VV energy transfer mechanism which becomes more specific and dominant at low energies.

In this study, we focus on the above mentioned VV and some selected VT processes that have been the topic of several experimental studies but for which no explicit quantum calculations have been reported. We employ a full quantum close coupling approach with an interaction potential that explicitly includes the stretching of the H_2 bond. Our previous studies of vibrational relaxation from $v = 1$ in H_2-H_2 collisions indicated that the full six-dimensional interaction potential of Hinde[36] yields results in closer agreement with experiment. Thus, we have chosen the Hinde potential for the calculations reported here. However, this interaction potential includes only a limited range for the H-H separation and it is not recommended for $v > 1$. Thus, our results presented here for $v = 2$ may not be as accurate as for $v = 1$. Nevertheless, our calculations provide improved agreement with experiments compared to the semiclassical calculations of Billing and co-workers[27–30] and illustrate the importance of quantum effects in VV and VT energy transfer processes in light molecules such as H_2. The paper is organized as follows: A

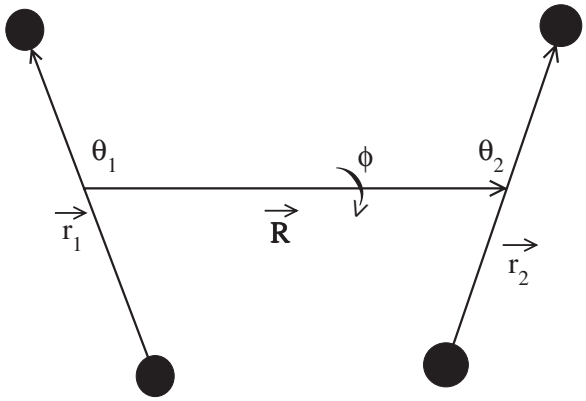

FIG. 1. Jacobi coordinates for the tetratomic system.

brief description of the methodology is provided in Sec. II. Results are given in Sec. III and further discussed in Sec. IV. Conclusions are presented in Sec. V.

II. THEORY AND COMPUTATIONAL DETAILS

A full close-coupling formalism based on the solution of the time-independent Schrödinger equation is used to solve the scattering problem. The scattering calculations are carried out using a modified version of the TwoBC code.[57] The modifications allow treatment of both distinguishable and indistinguishable molecules. Only a brief description of the methodology is presented here. A more detailed discussion can be found in Refs. 53 and 54 as well as in the work of Takayanagi,[58] Green,[59] Alexander and DePristo,[60] and Zarur and Rabitz.[61] The close-coupling formalism uses the total angular momentum space-fixed representation of Arthurs and Dalgarno[62] to solve the time-independent Schrödinger equation. Atomic units are used throughout, unless otherwise noted.

The Jacobi coordinate system employed in the calculations is shown in Fig. 1. The Hamiltonian,

$$H(\vec{r}_1, \vec{r}_2, \vec{R}) = T(\vec{r}_1) + T(\vec{r}_2) + T(\vec{R}) + V(\vec{r}_1, \vec{r}_2, \vec{R}) \tag{1}$$

of the four-atom system is composed of a kinetic energy term $T(\vec{R})$ describing the relative motion of the two molecules, two kinetic energy terms $T(\vec{r}_1)$ and $T(\vec{r}_2)$ for each diatomic molecule and the potential energy surface (PES) function,

$$V(\vec{r}_1, \vec{r}_2, \vec{R}) = U(\vec{r}_1, \vec{r}_2, \vec{R}) + V(\vec{r}_1) + V(\vec{r}_2) \tag{2}$$

describing the interaction between the two H_2 molecules. The kinetic energy terms of the Hamiltonian in Eq. (1) include contributions from the rotational motions of the two diatoms and the orbital angular momentum associated with the relative motion. Thus, the operator $H(\vec{r}_i) = T(\vec{r}_i) + V(\vec{r}_i)$, $i = 1, 2$ describes the rovibrational energies of the two molecules. For each value of the total angular momentum quantum number J and its projection M on a space-fixed axis, the diabatic functions

$$\phi_{vjl}^{JM}(\vec{r}_1, \vec{r}_2, \hat{R}) = \chi_{vj_1j_2}(r_1, r_2)\langle \hat{r}_1\hat{r}_2\hat{R}|jlJM\rangle \tag{3}$$

serve as basis functions to expand the total wave function

$$\Psi(\vec{r}_1, \vec{r}_2, \vec{R}) = \frac{1}{R}\sum_{v,j,l,J,M} F_{vjl}^{JM}(R)\phi_{vjl}^{JM}(\vec{r}_1, \vec{r}_2, \hat{R}). \tag{4}$$

The functions $\chi_{vj_1j_2}(r_1, r_2)$ denote the vibrational wave functions of the two molecules and $\langle \hat{r}_1\hat{r}_2\hat{R}|jlJM\rangle$ denote rotational wave functions in the total angular momentum representation. The subindexes v and j refer to the collection of vibrational (v_1, v_2) and rotational (j_1, j_2, j_{12}) quantum numbers, respectively. Explicit expressions for these quantities are given in Refs. 53 and 54.

Substitution of Eqs. (1) and (4) in the time-independent Schrödinger equation leads to a set of close-coupling radial equations,

$$\left\{-\frac{1}{2\mu}\frac{d^2}{dR^2} + \frac{l(l+1)}{2\mu R^2} + \varepsilon_{vj} - E\right\} F_{vjl}^{JM\varepsilon_I\varepsilon_P}(R) + \sum_{\lambda v'j'l'} \mathcal{U}_{vjl,v'j'l'}^{JM\varepsilon_I\varepsilon_P;\lambda}(R)F_{v'j'l'}^{JM\varepsilon_I\varepsilon_P}(R) = 0, \tag{5}$$

which are solved using the log-derivative method.[63,64] In the above expression, ε_{vj} denotes the rovibrational energy of the separated H_2 pairs corresponding to a given $|v, j\rangle = |v_1, j_1; v_2, j_2\rangle$ level. The inversion and exchange-permutation symmetries are represented by ε_I and ε_P, respectively.

For indistinguishable molecules, the state-to-state cross section is given by a statistically weighted sum of the exchange-permutation symmetrized cross sections

$$\sigma_{v_1j_1v_2j_2\to v_1'j_1'v_2'j_2'}(E_c) = W^+\sigma^{\varepsilon_P=+1} + W^-\sigma^{\varepsilon_P=-1} \tag{6}$$

with

$$\sigma^{\varepsilon_P=\pm1} = \frac{\pi(1+\delta_{v_1v_2}\delta_{j_1j_2})(1+\delta_{v_1'v_2'}\delta_{j_1'j_2'})}{(2j_1+1)(2j_2+1)k^2} \times \sum_{j_{12}j_{12}'}\sum_{ll'}\sum_{J}\sum_{\varepsilon_I}(2J+1) \times \left|\delta_{v_1j_1v_2j_2,v_1'j_1'v_2'j_2'} - S_{v_1j_1v_2j_2,v_1'j_1'v_2'j_2'}^{J\varepsilon_I\varepsilon_P=\pm1}(E_c)\right|^2, \tag{7}$$

where E_c is the center-of-mass kinetic energy for the initial channel. For para-H_2 molecules (nuclear spin $I = 0$), $W^+ = 1$ and $W^- = 0$. For ortho-H_2, $W^+ = 2/3$ and $W^- = 1/3$. Corresponding expressions for distinguishable molecules are given in Refs. 53 and 54.

The state-to-state rate coefficients are obtained by integrating the corresponding cross sections over the Maxwell-Boltzmann distribution of relative velocities,

$$k_{v_1j_1v_2j_2\to v_1'j_1'v_2'j_2'}(T) = \frac{1}{k_BT}\left(\frac{8}{\pi\mu k_BT}\right)^{1/2} \times \int_0^\infty \sigma_{v_1j_1v_2j_2\to v_1'j_1'v_2'j_2'}(E_c)e^{-E_c/(k_BT)}\,E_c\,dE_c. \tag{8}$$

The computational details of the calculations follow the description given in Refs. 13 and 53–55. A series of convergence tests determined the size of basis sets included in the expansion (4). Due to symmetry considerations, para-para H_2

TABLE I. The first and second columns show the choice of the basis set and the cut-off energies. In the first column o-H_2 and p-H_2 stands for ortho-H_2 and para-H_2, respectively. The basis set is denoted by the maximum rotational quantum number j included in each relevant vibrational level v of the H_2 molecule. For instance, for ortho-para H_2 {0,9;1,7-0,10;1,6} means that for the ortho-H_2 we have included rotational states up to $j_{v=0} = 9$ in the $v = 0$ vibrational level and $j_{v=1} = 7$ in $v = 1$. The third column shows the number of channels involved at each step of the calculations. Para-para and ortho-para H_2 require calculations for each inversion symmetry (positive and negative), while for ortho-ortho H_2 collisions, besides inversion, positive and negative exchange-permutation symmetries also need to be accounted for.

Basis set $\{v = 0, j_{v=0}; v = 1, j_{v=1}; v = 2, j_{v=2}\}$	Energy cut-off (cm^{-1})	No. of channels
from $v = 1$:		
p-H_2 - p-H_2 {0,10;1,6-0,10;1,6}	14 000	1 378 + 1 314 = 2 692
o-H_2 - o-H_2: {0,9;1,7-0,9;1,7}	14 000	1 238 + 1 228 + 1 277 + 1 228 = 4 971
o-H_2 - p-H_2: {0,9;1,7-0,10;1,6}	14 000	3 168 + 3 094 = 6 262
from $v = 2$:		
p-H_2 - p-H_2: {0,8;1,8;2,6-0,8;1,8;2,6}	16 000	1836[a] + 1 748 = 3 584
p-H_2 - o-H_2: {0,8;1,8;2,4-0,9;1,9;2,5}	16 000	4 098 + 3 991 = 8 089

[a]For $H_2(v_1 = 2, j_1 = 0) + H_2(v_2 = 0, j_2 = 0)$ only 1 836 channels.

calculations lead to a smaller basis set and, in turn, a much smaller set of coupled differential equations to be solved. On the other hand, ortho-ortho and ortho-para calculations are computationally more demanding requiring typically a few thousand coupled channels. We adopted an energy cut-off to minimize the number of coupled channels. The choice of the basis set and the energy cut-off reflects an effort to strike a balance between accuracy and computational efficiency. Our choices of basis set, the cut-off energy, and the number of channels for each case are given in Table I.

III. RESULTS

A. Cross sections

We present results for $H_2(v = 1–2)$ colliding with $H_2(v = 0)$ with rotational levels $j = 0–3$. For convenience, we use the notation $v_1 j_1 v_2 j_2$ for each state corresponding to a $H_2(v_1, j_1) + H_2(v_2, j_2)$ collision pair. Using this notation, the considered initial states are: 1001, 1201, 1301, 1103, 2000, 2001, and 2002. Results for 1301 and 1103 initial states have been reported in Ref. 55 and only comparison of their rate coefficients with experimental data will be discussed here. Extensive convergence tests have been carried out to verify that results (elastic and leading inelastic cross sections) presented are converged to within 5% or better with respect to the choice of the basis set, energy cut-off value, and summation over angular momentum partial waves. The collision energy range investigated spans from 1 μK to 10 000 K (6.9 $\times$ 10^{-7} to 6.9 $\times$ 10^3 cm^{-1}). In Figs. 2–6, we present the state-to-state cross sections for each of the initial states. Only cross sections for selected transitions are presented for clarity. State-to-state cross sections that are not included in the figures make negligible (<1%) contribution to the total inelastic cross section.

1. Rovibrational transitions from v = 1

Due to the different nuclear exchange-permutation symmetries of the colliding molecules (para- and ortho-H_2), no exchange of rotational quanta between the two molecules leading directly to an ortho-para transition can occur. However, as shown in Fig. 2, exchange of a vibrational quantum between the two molecules (1001 $\rightarrow$ 0011, a resonant VV transition) is the dominant inelastic transition for energies below 540 K. Above this energy, rotational excitation of the para-H_2 molecule leading to the 1201 final state becomes the dominant inelastic channel.

For the 1201 initial state, shown in Fig. 3, a VV exchange (1201 $\rightarrow$ 0211) is not the predominant inelastic process. In contrast to the 1001, a pure rotational de-excitation of the $v = 1$ molecule (1201 $\rightarrow$ 1001) dominates at low energies until a rotational excitation channel opens up leading to the population of the 1003, 1203, and 1401 final states. The final state 1003 involves simultaneous rotational de-excitation of the vibrationally excited para-H_2 molecule and rotational excitation of the vibrational ground state ortho-H_2 molecule. For both 1001 and 1201, the vibrational de-excitation (VT) channel makes negligible contribution to the total inelastic cross section.

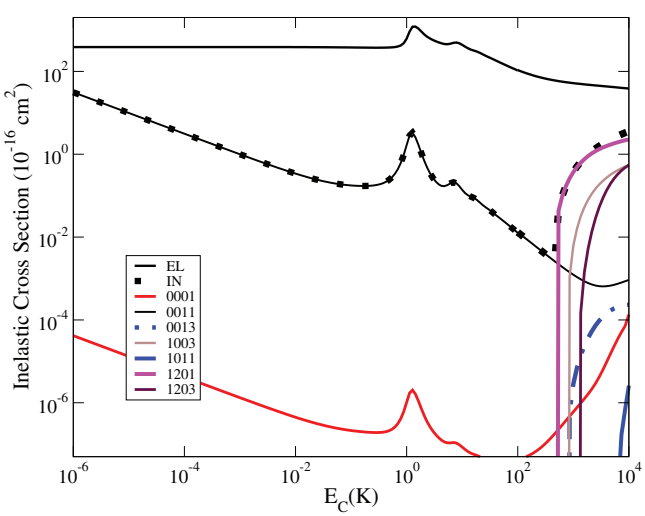

FIG. 2. Cross sections for the 1001 initial state as a function of the center-of-mass collision energy. The top curve denotes the elastic cross section and the thick dotted curve represents the total inelastic cross section. The main contribution to the inelastic process comes from the 0011 final state and, above 540 K, from the 1201 channel. Rotational transitions are more predominant than the VV transition at higher collision energies.

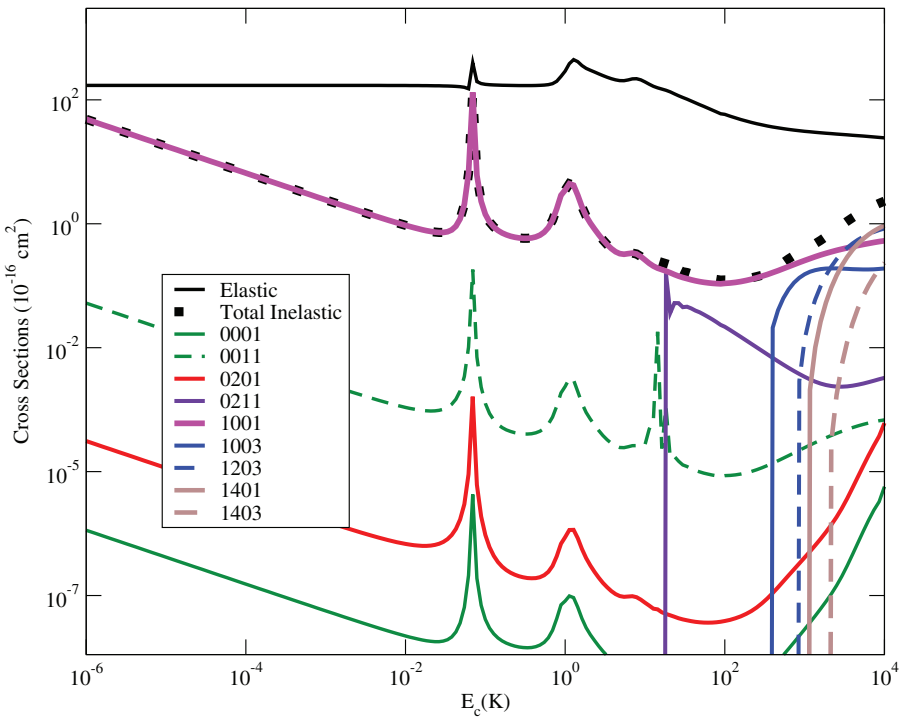

FIG. 3. Cross sections for the 1201 initial state as a function of the center-of-mass collision energy. As in Fig. 2, the top curve denotes the elastic cross section while the thick dotted curve represents the total inelastic cross section. The latter is dominated by the 1201 → 1001 transition. At higher energies, additional transitions involving rotational changes in one or both molecules make significant contributions to the inelastic cross section.

2. Rovibrational transitions from v=2

For $H_2(v=2\ j_1) + H_2(v=0\ j_2)$, the 2000, 2002, and 2001 initial states are considered. The 2001 para-ortho case turned out to be computationally very demanding, due to the need for a distinguishable basis set. Results for the 2000 initial state are shown in Fig. 4. Because of the indistinguishability of the molecules, the resonant VV transition 2000 → 0020 is incorporated in the elastic channel. At energies

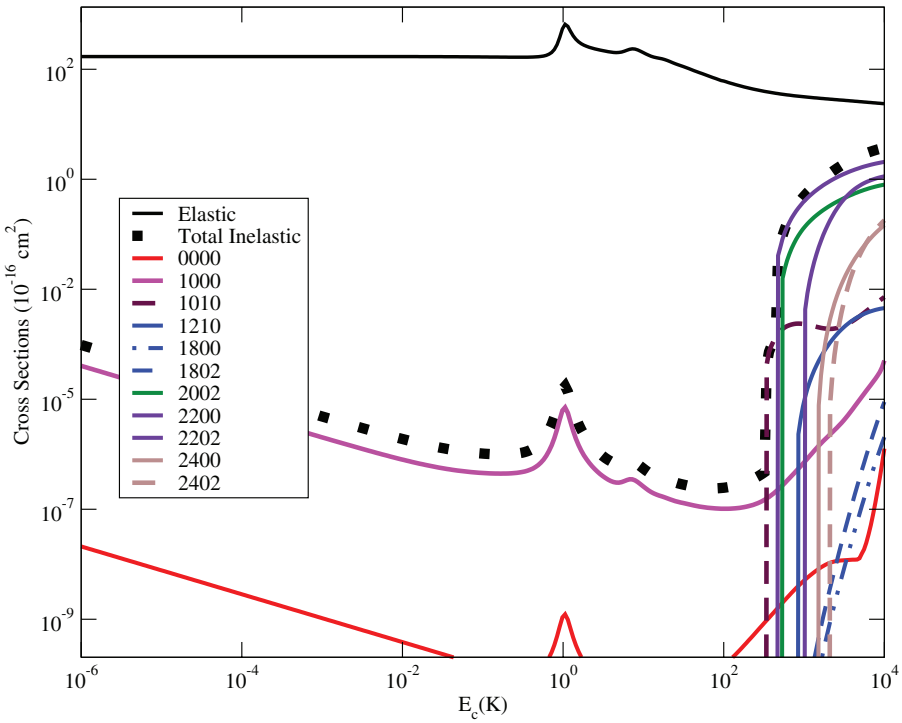

FIG. 4. Cross sections for the 2000 initial state as a function of the center-of-mass collision energy. The solid curve on the top represents the elastic cross section. The contribution to the total inelastic cross section (thick dotted curve) arises mainly from VT process (1000) at low energies and the VV process (1010) in the small window of 340-470 K. At higher energies, mainly rotational excitation contributes to the inelastic cross section.

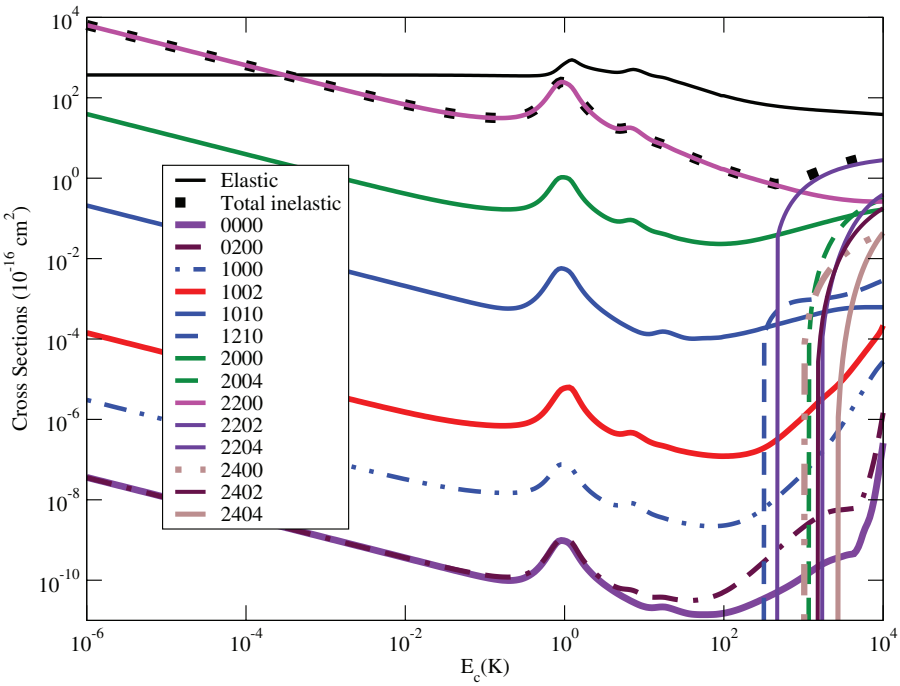

FIG. 5. Cross sections for the 2002 initial state as a function of the center-of-mass collision energy. The solid dark curve corresponds to the elastic cross section which dominates at energies above 3×10^{-4} K. The dominant inelastic channel is the quasi-resonant RR transition that leads to the 2200 final state. This process is equivalent to the QRRR transfer discussed in Ref. 55.

below 340 K, the inelastic cross section is dominated by the 2000 → 1000 VT transition. For the energy range 340–470 K, the non-resonant VV 2000 → 1010 transition is the primary inelastic channel. For higher energies, rotational excitations become more important.

The cross sections for the 2002 initial state are shown in Fig. 5. Due to the rotational de-excitation of the $v = 0$ molecule we are now able to discriminate the near-resonant RR transition 2002 → 2200. As expected, based on our previous results on para-para[13,53,54] and ortho-ortho[55] H_2-H_2

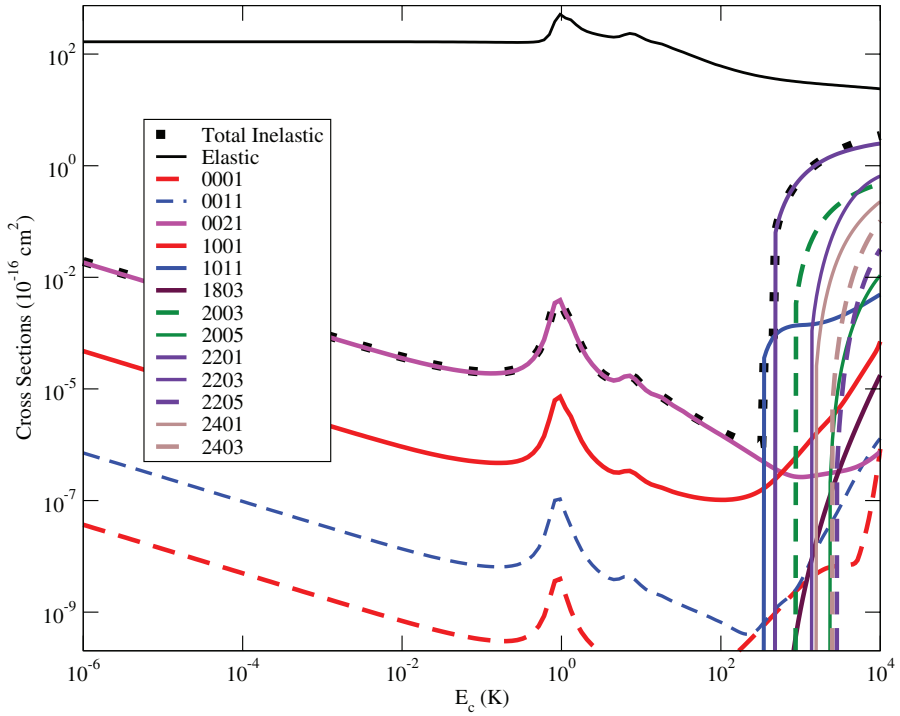

FIG. 6. Cross sections for the 2001 initial state as a function of the center-of-mass collision energy. As in Fig. 4, the total inelastic cross section has three different regions in which a single process dominates the cross section. This is comprised of the resonant VV transition 2001 → 0021, followed by the non-resonant 2001 → 1011 VV transition, and finally, the rotational excitation channels.

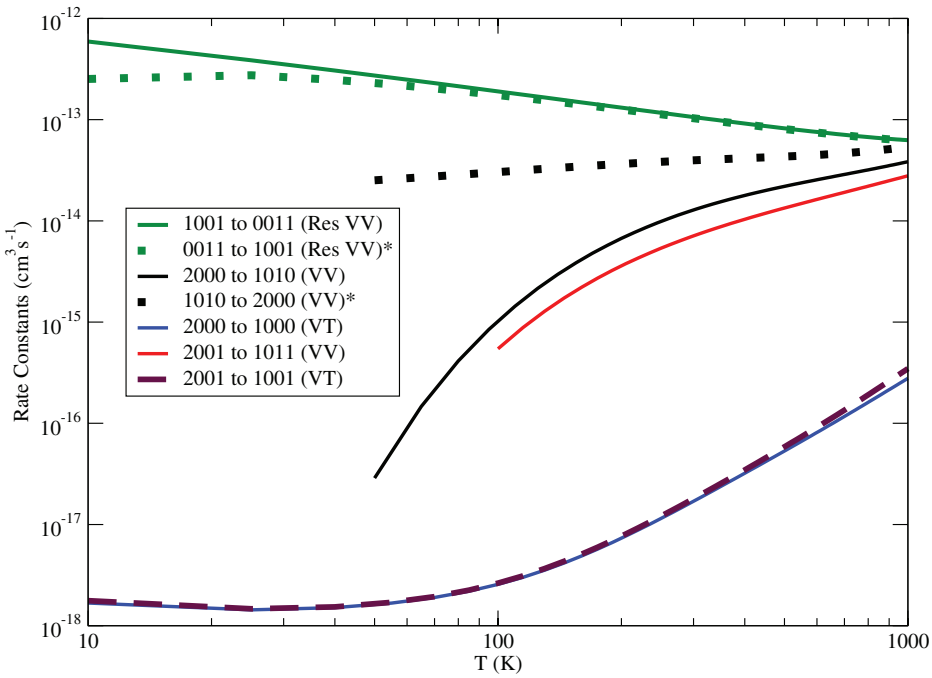

FIG. 7. Rate constants for different VV and VT transitions as functions of the temperature. The symbol "*" on the legend of the 0011 → 1001 and 1010 → 2000 indicates that the curves were obtained by detailed balance from the 1001 → 1100 and 2000 → 1010 transitions, respectively. The acronyms in parenthesis, VT and VV denote vibration-translation and vibration-vibration transitions, while Res VV denotes resonant VV transition.

collisions, this quasi-resonant process (referred to as QRRR-quasi-resonat rotation-rotation transition in Ref. 55) dominates over all the other inelastic channels in the cold and ultracold energy regime. Similar to the 2000 case, at about 470 K, the 2002 → 2202 transition (pure rotational excitation) becomes energetically accessible and dominates the inelastic cross section. On the other hand, the 2002 → 1002 VT transition contributes less than 1% to the total inelastic cross section.

The cross sections for $H_2(v=2\ j=0) + H_2(v=0\ j=1)$ collisions (2001) are shown in Fig. 6. The resonant VV transition, 2001 → 0021, which involves the exchange of two vibrational quanta between the two molecules, is the dominant inelastic channel for energies below 300 K. This is followed by the 2001 → 1011 transition which involves the exchange of one vibrational quantum. Beyond a collision energy of 485 K, the rotational excitation channels become more predominant.

B. Rate coefficients

Rate coefficients for some state-to-state transitions are shown in Fig. 7. The 0011 → 1001 and 1010 → 2000 transition rate coefficients were obtained by detailed balance (see for instance Ref. 38). It is seen that the rate coefficients for the resonant VV transition, 1001 → 0011, and the reverse process are nearly identical for the displayed temperature range. This is attributed to the very small energy defect of only 8.5 K between these states. The second set of curves correspond to the non-resonant VV transitions 2000 → 1010 and its reverse process. The energy defect for these transitions is about 340 K with the 1010 → 2000 being the exothermic direction. The dotted curve corresponds to the 2001 → 1011 VV transition. The bottom two curves correspond to the 2000 → 1000 and 2001 → 1001 VT transitions. It is clear that the rate coefficients for the VV transitions are much greater than that of the VT transitions.

IV. DISCUSSION

Rate coefficients for selected transitions from our calculations are presented in Table II along with available theoretical and experimental results. For the 1001 → 0011 transition, which occurs through a VV process, Farrow and Chandler[24] reported a value of $7.1 \pm 3 \times 10^{-14}$ cm^3 s^{-1} at 298 K which is in agreement with our computed value of 1.05×10^{-13} cm^3 s^{-1}. Our rate coefficient for the reverse process, 0011 → 1001, estimated from detailed balance, is 1.0×10^{-13} cm^3 s^{-1} at 300 K, in excellent agreement with the experimental result of $9.9 \pm 2 \times 10^{-14}$ cm^3 s^{-1} reported by Ahn *et al.*[26] Our result is also in close agreement with the value of 1.2×10^{-13} cm^3 s^{-1} reported by Kelly[31] using a semiclassical approach that treats both rotational and vibrational motions quantum mechanically. In contrast, the semiclassical result of Cacchiatore and Billing[28] is 3.6×10^{-15} cm^3 s^{-1}, about a factor of 28 smaller. The discrepancy is, in part, attributed to the classical treatment of rotational motion which is not adequate for a light molecule such as H_2.

Meier *et al.*[22] reported experimental rate coefficients for $H_2(v_1=1, j_1=1) + H_2(v_2=0, j_2)$ collisions. However, it is not clear if the H_2 molecule in the $v=0$ level is ortho-H_2 or normal-H_2. They reported rate coefficients for rotational excitation corresponding to the $j_1 = 1 \rightarrow 3$ transition, $H_2(v_1=1, j_1=1) + H_2(v_2=0, j_2) \rightarrow H_2(v_1=1, j_1=3) + H_2(v_2=0, j_2)$ (referred to as k_{13}), and its reverse

TABLE II. Comparison of H_2-H_2 rate coefficients for different transitions from the present study and available experimental and theoretical data.

T (K)	$v_1 j_1 v_2 j_2 \rightarrow v_1' j_1' v_2' j_2'$	$k(T)$ (cm^3/s) This work	$k(T)$ (cm^3/s)
298	1001 → 0011	1.07×10^{-13}	$7.1 \pm 3 \times 10^{-14}$ (Ref. 24)
298	0011 → 1001	1.04×10^{-13}	1.2×10^{-13} (Ref. 31)
298	1201 → 0211	9.83×10^{-14}	...
298	0211 → 1201	1.04×10^{-13}	1.3×10^{-13} (Ref. 31)
300	1101 → 1301	3.54×10^{-13}	2.3×10^{-12} (Ref. 22)
300	1301 → 1101	2.20×10^{-12}	14.3×10^{-12} (Ref. 22)
298	2000 → 1010	1.28×10^{-14}	(1-4) $\times 10^{-14}$ (Ref. 23)
300	1010 → 2000	3.98×10^{-14}	$3.8 \pm 0.8 \times 10^{-14}$ (Ref. 26)
300	2000 → 1000	1.70×10^{-17}	...
300	2001 → 1011	7.11×10^{-15}	...
298	2001 → 1001	1.78×10^{-17}	(0.6-2) $\times 10^{-15}$ (Ref. 23)

process k_{31}. As discussed by Meier *et al.*,[22] their experiments could not discriminate $H_2(v_1 = 1, j_1 = 3)$ formed through an additional channel, $H_2(v_1 = 1, j_1 = 1) + H_2(v_2 = 0, j_2) \rightarrow H_2(v_1 = 1, j_1 + \Delta j) + H_2(v_2 = 0, j_2 - \Delta j)$. If $j_2 = 3$, this would correspond to a 1103 → 1301 transition, which can also occur through exchange of rotational quanta between the two molecules. The value of k_{13} reported in their study includes contributions from both processes. Our calculation yields a rate coefficient of 3.54×10^{-13} cm^3 s^{-1} for the 1101 → 1301 transition at 300 K compared to the value of 2.3×10^{-12} cm^3 s^{-1} reported by Meier *et al.*[22] for k_{13}. For the reverse process, Meier *et al.*[22] reported a value of $k_{31} = 14.3 \times 10^{-12}$ cm^3 s^{-1}. Our calculations yield a rate coefficient of 2.2×10^{-12} cm^3 s^{-1} for the 1301 → 1101 transition. Thus, our results are about a factor of 6.5 smaller than experiment for both k_{13} and k_{31}. However, it must be emphasized that, as discussed in detail in our previous publication,[55] in $H_2(v_1 = 1, j_1 = 3) + H_2(v_2 = 0, j_2 = 1)$ (1301) collisions the dominant final channel is 1103, corresponding to an exchange of rotational quanta between the two molecules or equivalently, rotational excitation of the $v = 0$ molecule and rotational quenching of the $v = 1$ molecule. The energy threshold for this process is 42.24 K. At 300 K, the rate coefficient for the 1301 → 1103 transition is 12.07×10^{-12} cm^3 s^{-1}. Thus, the sum of the rate coefficients for the two processes (1301 → 1101 and 1301 → 1103) becomes 14.27×10^{-12} cm^3 s^{-1}, in close agreement with experiment, if indeed the experimental rate coefficient includes both processes (note that the measurement does not distinguish these two processes as both lead to rotational relaxation of the vibrationally excited molecule, similar to rotational excitation of the $v = 1$ molecule discussed in the case of k_{13}).

Table II also lists rate coefficients for VV and VT transfer involving the $v = 2$ vibrational level for both ortho and para-H_2. For para-H_2, the 2000 → 1010 VV rate coefficient is 1.28×10^{-14} cm^3 s^{-1} at 300 K. The corresponding 2000 → 1000 VT rate coefficient is about two orders of magnitude smaller, at 1.7×10^{-17} cm^3 s^{-1} at 300 K. Kreutz *et al.*[23] reported experimental results of VV and VT rate coefficients for $H_2(v = 2) + H_2(v = 0)$ collisions. For the VV process they reported a value of (1-4) $\times 10^{-14}$ cm^3 s^{-1} at 298 K compared to a value of (0.6-2) $\times 10^{-15}$ cm^3 s^{-1} for the VT counterpart. In a more recent experiment, Ahn *et al.*[26] reported experimental results for the VV process to be 1.3×10^{-14} cm^3 s^{-1} in excellent agreement with our predicted value. While our results for the VV process is in close agreement with experiment, our predicted value for the VT rate coefficient is about an order of magnitude smaller than measured. However, it is important to emphasize that the computed result pertains to specific rovibrational transitions for para-H_2, while the measurements include a thermal population of rotational levels of both ortho- and para-H_2 molecules. Since VT rates are much smaller, they are much more sensitive to the details of the interaction potential and initial population of rotational levels. Nevertheless, the important aspect is that both experiments and calculations indicate that the VV process is about an order of magnitude more efficient than the VT process. It is also interesting to note that the rate coefficient for this VV process (2000 → 1010) is about an order of magnitude smaller than the 1001 → 0011 VV process discussed above. The difference is attributed to the almost resonant character of the latter process (energy gap is only 8.5 K and the process is in the exothermic direction) compared to the non-resonant nature of the former (energy gap is 340 K and the process is in the endothermic direction). From detailed balance, we obtain a value of 3.98×10^{-14} cm^3 s^{-1} for the 1010 → 2000 VV transition at 300 K. This is in excellent agreement with the experimental result of 3.8×10^{-14} cm^3 s^{-1} reported by Ahn *et al.*[26]

Finally, while it is noted above that ortho-para transitions for a given H_2 molecule are forbidden in the purely inelastic processes studied here, the 1001 → 0011 VV transition results in an effective $j = 1 \rightarrow j = 0$ conversion in $v = 0$. This is particularly intriguing as the rate coefficient, shown in Fig. 7, is large and slightly increasing with decreasing temperature, as it is exothermic by 8.5 K. A similar effect occurs for 1201 → 0011, but because the energy gap is 493 K, it is less efficient by two orders of magnitude. The 1201 → 0211 transition, on the other hand, is efficient, driving an effective $v = 0, j = 1 \rightarrow j = 2$ conversion, though it is endothermic by 17 K. Such mechanisms may be important in molecular gas when the abundance of atomic hydrogen is too small to drive H_2 ortho-para conversions through reactive channels.

V. CONCLUSION

Detailed state-to-state cross sections and rate coefficients for rotational and vibrational energy transfer in H_2-H_2 collisions with an emphasis on VV and VT transfer process are presented. The primary motivation of these studies is to provide a full quantum mechanical description of these processes on a reliable, full-dimensional potential energy surface so that benchmark results can be obtained for comparison with available experimental data and future investigations. Our calculations show that the VV process is about an order of magnitude more efficient than VT transitions, in agreement with available experimental data. In $H_2(v = 1, j = 0) + H_2(v = 0, j = 1)$ (1001) collisions, the resonant VV transition leading to $H_2(v = 0, j = 0) + H_2(v = 1, j = 1)$ (0011) products dominates over pure vibrational relaxation of the para-H_2 molecule. Similarly, in $H_2(v = 2, j = 0) + H_2(v = 0, j = 0)$ (2000) collisions VV transfer leading to $H_2(v = 1, j = 0) + H_2(v = 1, j = 0)$ (1010) products dominate over VT process leading to the $H_2(v = 1, j = 0) + H_2(v = 0, j = 0)$ (1000) channel. Due to the almost resonant character of the $1001 \rightarrow 0011$ VV transfer, its rate coefficient is found to be about an order of magnitude larger than the non-resonant $2000 \rightarrow 1010$ VV transition. Our results are in excellent agreement with experiment for both the $2000 \rightarrow 1010$ process and its reverse exoergic counterpart. The current full quantum dynamics calculations are also in close agreement with the semiclassical results of Kelly,[31] who adopted a quantum mechanical approach for both the rotational and vibrational degrees of freedom, but treated the relative motion classically.

The coupled channel formalism employed in the calculations can be applied to excited vibrational levels of H_2 beyond the $v = 0$-2 levels considered in this study. Unfortunately, the PES adopted here is not recommended for high vibrational levels and we hope that improved calculations of the H_2-H_2 interaction potential will allow investigations of energy transfer mechanism in highly vibrationally excited H_2.

ACKNOWLEDGMENTS

This work was supported by NSF grants PHY-1205838, (N.B.), ATM-0635715 (N.B.), PHY-1203228 (R.C.F.), and AST-0607733 (P.C.S.). This research was supported in part by NSF through XSEDE resources provided by the National Institute for Computational Sciences through Grant No. CHE100039 (N.B.).

[1] K. S. Kalogerakis, G. P. Smith, and R. A. Copeland, J. Geophys. Res. **116**, D20307, doi:10.1029/2011JD015734 (2011).
[2] W.-F. Thi, E. F. van Dishoeck, K. M. Pontoppidan, and E. Dartois, Mon. Not. R. Astron. Soc. **406**, 1409 (2010).
[3] P. Vankan, D. C. Schram, and R. Engeln, J. Chem. Phys. **121**, 9876 (2004).
[4] L. D. Carr, D. DeMille, R. V. Krems, and J. Ye, New J. Phys. **11**, 055049 (2009).
[5] G. Quéméner, N. Balakrishnan, and A. Dalgarno, in *Cold Molecules: Theory, Experiment, Applications*, edited by R. Krems, W. C. Stwalley, and B. Friedrich (CRC, 2009), pp. 69–124.
[6] G. Quéméner and P. S. Julienne, Chem. Rev. **112**, 4949 (2012).
[7] N. R. Hutzler, H.-I. Lu, and J. M. Doyle, Chem. Rev. **112**, 4803 (2012).
[8] S. Y. T. van de Meerakker, H. L. Bethlem, N. Vanhaecke, and G. Meijer, Chem. Rev. **112**, 4828 (2012).
[9] R. Wynar, R. S. Freeland, D. J. Han, C. Ryu, and D. J. Heinzen, Science **287**, 1016 (2000).
[10] P. Courteille, R. S. Freeland, D. J. Heinzen, F. A. van Abeelen, and B. J. Verhaar, Phys. Rev. Lett. **81**, 69 (1998).
[11] C. Chin, R. Grimm, P. Julienne, and E. Tiesinga, Rev. Mod. Phys. **82**, 1225 (2010).
[12] N. Balakrishnan, R. C. Forrey, and A. Dalgarno, Phys. Rev. Lett. **80**, 3224 (1998).
[13] G. Quéméner, N. Balakrishnan, and R. V. Krems, Phys. Rev. A **77**, 030704(R) (2008).
[14] *Molecular Hydrogen in Space*, edited by F. Combes and G. Pineau des Forêts (Cambridge University Press, 2000).
[15] K. Hassouni, A. Gicquel, M. Capitelli, and J. Loureiro, Plasma Sources Sci. Technol. **8**, 494 (1999).
[16] M. J. de Graaf, R. Severens, R. P. Dahiya, M. C. M. van de Sanden, and D. C. Schram, Phys. Rev. E **48**, 2098 (1993).
[17] P. S. Krstić, D. R. Schultz, and R. K. Janev, Phys. Scr. **T96**, 61 (2002).
[18] P. S. Krstić, Phys. Rev. A **66**, 042717 (2002).
[19] D. W. Savin, P. S. Krstić, Z. Haiman, and P. C. Stancil, Astrophys. J. **606**, L167 (2004); erratum **607**, L147 (2004).
[20] S. C. O. Glover and T. Abel, Mon. Not. R. Astron. Soc. **388**, 1627 (2008).
[21] M.-M. Audibert, R. Vilaseca, J. Lukasik, and J. Ducuing, Chem. Phys. Lett. **31**, 232 (1975).
[22] W. Meier, G. Ahlers, and H. Zacharias, J. Chem. Phys. **85**, 2599 (1986).
[23] T. G. Kreutz, J. Gelfand, R. B. Miles, and H. Rabitz, Chem. Phys. **124**, 359 (1988).
[24] R. L. Farrow and D. W. Chandler, J. Chem. Phys. **89**, 1994 (1988).
[25] B. Maté, F. Thibault, G. Tejeda, J. M. Fernández, and S. Montero, J. Chem. Phys. **122**, 064313 (2005).
[26] T. Ahn, I. Adamovich, and W. R. Lempert, Chem. Phys. **335**, 55 (2007).
[27] G. D. Billing and E. R. Fisher, Chem. Phys. **18**, 225 (1976).
[28] M. Cacciatore and G. D. Billing, J. Phys. Chem. **96**, 217 (1992).
[29] R. E. Kolesnick and G. D. Billing, Chem. Phys. **170**, 201 (1993).
[30] G. D. Billing and R. E. Kolesnick, Chem. Phys. Lett. **215**, 571 (1993).
[31] J. D. Kelley, J. Phys. Chem. **113**, 1995 (2009).
[32] D. W. Schwenke, J. Chem. Phys. **89**, 2076 (1988).
[33] A. Aguado, C. Suárez, and M. Paniagua, J. Chem. Phys. **101**, 4004 (1994).
[34] P. Diep and J. K. Johnson, J. Chem. Phys. **112**, 4465 (2000).
[35] A. I. Boothroyd, P. G. Martin, W. J. Keogh, and M. J. Peterson, J. Chem. Phys. **116**, 666 (2002).
[36] R. J. Hinde, J. Chem. Phys. **128**, 154308 (2008).
[37] K. Patkowski, W. Cencek, P. Jankowski, K. Szalewicz, J. B. Mehl, G. Garberoglio, and A. H. Harvey, J. Chem. Phys. **129**, 094304 (2008).
[38] D. R. Flower and E. Roueff, J. Phys. B **31**, 2935 (1998).
[39] D. R. Flower, Mon. Not. R. Astron. Soc. **297**, 334 (1998).
[40] D. R. Flower and E. Roueff, J. Phys. B **32**, 3399 (1999).
[41] D. R. Flower, J. Phys. B **33**, L193 (2000).
[42] D. R. Flower, J. Phys. B **33**, 5243 (2000).
[43] R. C. Forrey, Phys. Rev. A **63**, 051403(R) (2001).
[44] S. K. Pogrebnya and D. C. Clary, Chem. Phys. Lett. **363**, 523 (2002).
[45] S. Y. Lin and H. Guo, J. Chem. Phys. **117**, 5183 (2002).
[46] S. K. Pogrebnya, M. E. Mandy, and D. C. Clary, Int. J. Mass. Spectrom. **223–224**, 335 (2003).
[47] S. Y. Lin and H. Guo, Chem. Phys. **289**, 191 (2003).
[48] T.-G. Lee, N. Balakrishnan, R. C. Forrey, P. C. Stancil, D. R. Schultz, and G. J. Ferland, J. Chem. Phys. **125**, 114302 (2006).
[49] F. Gatti, F. Otto, S. Sukiasyan, and H.-D. Meyer, J. Chem. Phys. **123**, 174311 (2005).
[50] A. N. Panda, F. Otto, F. Gatti, and H.-D. Meyer, J. Chem. Phys. **127**, 114310 (2007).
[51] F. Otto, F. Gatti, and H.-D. Meyer, J. Chem. Phys. **128**, 064305 (2008).
[52] F. Otto, F. Gatti, and H.-D. Meyer, J. Chem. Phys. **131**, 049901 (2009).
[53] G. Quéméner and N. Balakrishnan, J. Chem. Phys. **130**, 114303 (2009).
[54] N. Balakrishnan, G. Quéméner, R. C. Forrey, R. J. Hinde, and P. C. Stancil, J. Chem. Phys. **134**, 014301 (2011).
[55] S. Fonseca dos Santos, N. Balakrishnan, S. Lepp, G. Quemener, R. C. Forrey, R. J. Hinde, and P. C. Stancil, J. Chem. Phys. **134**, 214303 (2011).
[56] B. Yang, R. C. Forrey, P. C. Stancil, S. Fonseca dos Santos, and N. Balakrishnan, Phys. Rev. Lett. **109**, 233201 (2012).
[57] R. V. Krems, TwoBC, quantum scattering program, University of British Columbia, Vancouver, Canada, 2006.

[58]K. Takayanagi, Adv. At. Mol. Phys. **1**, 149 (1965).
[59]S. Green, J. Chem. Phys. **62**, 2271 (1975).
[60]M. H. Alexander and A. E. DePristo, J. Chem. Phys. **66**, 2166 (1977).
[61]G. Zarur and H. Rabitz, J. Chem. Phys. **60**, 2057 (1974).
[62]A. M. Arthurs and A. Dalgarno, Proc. R. Soc. London, Ser. A **256**, 540 (1960).
[63]B. R. Johnson, J. Comput. Phys. **13**, 445 (1973).
[64]D. E. Manolopoulos, J. Chem. Phys. **85**, 6425 (1986).